Kraut, J. (1988) *Science 242*, 534–560.
Lakowicz, J. R. (1983) in *Principles of Fluorescence Spectroscopy*, Plenum Press, New York.
Levitt, M., & Sharon, R. (1988) *Proc. Natl. Acad. Sci. U.S.A. 85*, 7557–7561.
London, R. E., Howell, E. E., Warren, M. S., Kraut, J., & Blakley, R. L. (1986) *Biochemistry 25*, 7229–7235.
Lim, E. C. (1986) *J. Phys. Chem. 90*, 6770–6777.
Magde, D., & Campbell, B. F. (1989) *Proc. SPIE 154, Fluorescence Detection III*, 61–68.
Maggiora, G., Johansen, H., & Ingraham, L. L. (1969) *Arch. Biochem. Biophys. 131*, 352.
Maharaj, G., Selinsky, B. S., Appleman, J. R., Perlman, London, R. E., & Blakley, R. L. (1990) *Biochemistry 29*, 4554–4560.
Matthews, D. A., Alden, R. A., Bolin, J. T., Freer, S. T., Hamlin, R., Xuong, N., Kraut, J., Poe, M., Williams, M., & Hoogsteen, K. (1977) *Science 197*, 452–455.
Matthews, D. A., Bolin, J. T., Burridge, J. M., Filman, D. J., Volz, K. W., Kaufner, B. T., Beddill, C. R., Champness, J. N., Stammers, D. K., & Kraut, J. (1985) *J. Biol. Chem. 260*, 381–391.
McCammon, J. A., Gelin, B. R., & Karplus, M. (1977) *Nature 267*, 585–590.
Morrison, J. F., & Stone, S. R. (1988) *Biochemistry 27*, 5499–5506.
Northrup, D. B. (1977) in *Isotope Effects in Enzyme Catalyzed Reactions* (Cleland, W. W., Ed.) University Park Press, Baltimore, MD.
Osaki, A. Y., King, R. W., & Carey, P. R. (1981) *Biochemistry 20*, 3219–3225.
Poe, M., Greenfield, N. J., Hirshfield, J. M., & Hoogsteen, K. (1974) *Cancer Biochem. Biophys. 1*, 7–11.
Rojas, G., & Magde, D. (1983) *Chem. Phys. Lett. 102*, 399–403.
Saperstein, D. D., Rein, A. J., Poe, M., & Leahy, M. F. (1978) *J. Am. Chem. Soc. 100*, 4296–4300.
Scott, T. G., Spencer, R. D., Leonard, N. J., & Weber, G. (1970) *J. Am. Chem. Soc. 92*, 687–695.
Searle, M. S., Forster, M. J., Birdsall, B., Roberts, G. C. K., Feeney, J., Cheung, H. T. A., Kompis, I., & Geddes, J. (1988) *Proc. Natl. Acad. Sci. U.S.A. 85*, 3787–3791.
Seng, G., & Bolard, J. (1983) *Biochimie 65*, 169–75.
Villafranca, J. E., Howell, E. E., Voet, D. H., Strobel, M. S., Ogden, R. C., Abelson, J. N., & Kraut, J. (1983) *Science 222*, 782–788.
Visser, A. J. W. G., & van Hoek, A. (1981) *Photochem. Photobiol. 47*, 201–205.
Waldman, A. D. B., Hart, K. W., Clarke, A. R., Wigley, D. B., Barstow, D. A., Atkinson, T., Chia, W. N., & Holbrook, J. J. (1988) *Biochem. Biophys. Res. Commun. 150*, 752–759.
Yue, K. T., Martin, C. L., Chen, D., Nelson, P., Sloan, D. L., & Callender, R. H. (1986) *Biochemistry 25*, 4941–4947.

Q-Band ENDOR Spectra of the Rieske Protein from *Rhodobactor capsulatus* Ubiquinol–Cytochrome *c* Oxidoreductase Show Two Histidines Coordinated to the [2Fe–2S] Cluster†

Ryszard J. Gurbiel,‡,§ Tomoko Ohnishi,*,‖ Dan E. Robertson,‖ Fevzi Daldal,⊥ and Brian M. Hoffman*,‡

Department of Chemistry, Northwestern University, Evanston, Illinois 60208, Institute of Molecular Biology, Jagiellonian University, Krakow, Poland, and Department of Biochemistry and Biophysics and Department of Biology, University of Pennsylvania, Philadelphia, Pennsylvania 19104

Received June 19, 1991; Revised Manuscript Received August 27, 1991

ABSTRACT: Electron nuclear double resonance (ENDOR) experiments were performed on ^{14}N (natural abundance) and ^{15}N-enriched iron–sulfur Rieske protein in the ubiquinol–cytochrome c_2 oxidoreductase from *Rhodobactor capsulatus*. The experiments proved that two distinct nitrogenous ligands, histidines, are undoubtedly ligated to the Rieske [2Fe–2S] center. The calculations of hyperfine tensors give values similar but not identical to those of the Rieske-type cluster in phthalate dioxygenase of *Pseudomonas cepacia* and suggest a slightly different geometry of the iron–sulfur cluster in the two proteins.

A protein containing a [2Fe–2S] iron–sulfur cluster and generally called the Rieske iron–sulfur protein was first isolated from the ubiquinol–cytochrome *c* oxidoreductase (cytochrome bc_1) of bovine heart mitochondria (Rieske, 1976). Its functional role as the primary electron acceptor of ubiquinol in the bc_1 complex, and as the electron donor to cytochrome c_1, is well accepted (Trumpower, 1981). Rieske iron–sulfur proteins have been found to be distributed in a variety of respiratory systems, such as the cytochrome bc_1 complex of photosynthetic and nonphotosynthetic bacteria (Bowyer et al., 1980; Meinhardt et al., 1987) and the cytochrome b_6f complex of chloroplasts and cyanobacteria. These cytochrome complexes contain two *b* hemes, one c_1 (or *f* in b_6f), and one Rieske iron–sulfur cluster. In all cases, the Rieske iron–sulfur cluster exhibits an EPR spectrum that is more anisotropic and

† This work was supported by NIH Grants HL 1353 (B.M.H.), GM 38237 (F.D.), and 27309 and by NSF Grants DMB 8907559 (B.M.H.) and DMB 8819305 (T.O.).
* To whom correspondence should be addressed.
‡ Northwestern University.
§ Jagiellonian University.
‖ Department of Biochemistry and Biophysics, University of Pennsylvania.
⊥ Department of Biology, University of Pennsylvania.

0006-2960/91/0430-11579$02.50/0

characterized by a lower g_{av} ($g_1 \simeq 2.02$, $g_2 \simeq 1.90$, $g_3 \simeq 1.80$, and $g_{av} \simeq 1.91$) than that of typical ferredoxin-type [2Fe–2S] clusters, where $g_{av} \simeq 1.96$. The Rieske-type clusters also exhibit high redox midpoint potentials (150–330 mV) relative to the low E_m values ($\simeq$ −300 to −400 mV) of typical ferredoxins (Yasunobu & Tanaka, 1977; Trumpower, 1981). This $g_{av} \simeq 1.91$ type of iron–sulfur cluster is not only associated with the cytochrome bc_1 of mitochondrial, chloroplast, and bacterial respiratory chains but is also found in mono- and dioxygenases of certain bacteria, exemplified by *Pseudomonas cepacia* phthalate dioxygenase (Batie et al., 1987).

Blumberg and Peisach (1974) devised a method of EPR spectral interpretation of reduced binuclear clusters that led them to suggest that Rieske-type iron–sulfur clusters may include terminal ligand(s) less electron donating than sulfur. In 1984, Fee and his collaborators reported the first experimental evidence indicating the involvement of two non-sulfur ligands in the Rieske-type [2Fe–2S] cluster, on the basis of the chemical, EPR, and Mössbauer analyses of a Rieske-type protein isolated from the *Thermus thermophilus* HB-8 cells. The combined data indicated that this Rieske-type protein contains two identical [2Fe–2S] clusters per molecule (20 kDa) and that the two non-sulfur ligands are coordinated to both clusters, possibly at the Fe^{2+} site. Subsequently, Cline et al. (1985) conducted X-band ENDOR[1] and ESEEM analysis of the Rieske-type protein isolated from *T. thermophilus* HB-8 cells and *P. cepacia* PDO and detected signals arising from ^{14}N (natural abundance). Similar ENDOR and ESEEM data were obtained on the Rieske [2Fe–2S] cluster of yeast ubiquinol–cytochrome *c* oxidoreductase (Telser et al., 1987).

Recently, Gurbiel et al. (1989) reported a more rigorous analysis of ENDOR data of the Rieske-type [2Fe–2S] cluster of phthalate dioxygenase of *P. cepacia*. The experiments, performed at both X-band (9 GHz) and Q-band (35 GHz) employed enzyme isolated from cells grown in either ^{14}N- or ^{15}N-enriched media, as well as enzyme isolated from histidine auxotrophs grown on [^{15}N]- or [^{14}N]histidine with a ^{14}N or ^{15}N background. These studies clearly demonstrated that two magnetically distinct nitrogen ligands from two histidine residues are coordinated to the [2Fe–2S] cluster. This contrasts with classical ferredoxin-type [2Fe–2S] clusters in which all ligation is provided by the sulfur of cysteine residues (Fukuyama et al., 1980). The detailed analysis of the polycrystalline data allowed, for each nitrogen ligand, determination of the principal values of the hyperfine tensor and its orientation with respect to the *g* tensor, as well as the ^{14}N quadrupole coupling tensor. The combination of these results with earlier Mössbauer and resonance Raman studies supports a model for the reduced cluster with both histidyl ligands bound to the ferrous ion of the spin-coupled [Fe^{2+} (S = 2), Fe^{3+} (S = 5/2)] pair. The analysis of hyperfine and quadrupole tensors indicates that the geometry of ligation at Fe^{2+} is approximately tetrahedral, with the Fe_2N_2 plane corresponding to the g_1–g_3 plane.

Nevertheless, recent studies of amino acid sequence homology of the respiratory chain Rieske iron–sulfur proteins have been interpreted differently. Data from 10 different sources have revealed full conservation of four cysteine and two histidine residues (^{129}C-T-H-L-G-C-V-...-^{148}C-P-C-H-G; the numbers are from the Rieske protein of *Saccharomyces cerevisiae*) in close proximity to the C-terminus (Harnish et al., 1085; Davidson & Daldal, 1987; Trumpower, 1990). On the basis of the analysis of 11 respiratory deficient yeast mutants with a single amino acid replacement, Gatti et al. (1989) suggested that the Rieske iron–sulfur cluster in yeast mitochondria is ligated by three cysteine residues and one histidine. Furthermore, EXAFS studies of the Rieske protein isolated from the cytochrome bc_1 complex of bovine heart mitochondria (Powers et al. 1989) favored a ligand set of three sulfur and one nitrogen for the [2Fe–2S] cluster, although the possibility of the two sulfur and two nitrogen ligands could not be completely excluded.

To resolve this long standing issue of Rieske cluster ligation, we have examined the ligand structure of the Rieske iron–sulfur cluster in cytochrome bc_1 utilizing the ^{15}N-enriched overproduced *Rhodobactor capsulatus* system (BC1) combined with the Q-band ENDOR technique. The results demonstrate the presence of two nitrogen ligands. The characteristics of the ligands and the inferred structure of the cluster are compared with that of the Rieske-type iron–sulfur cluster in the *P. cepacia* system (PDO). Results from ESEEM measurements on a series of Rieske proteins seem to be consistent with the picture discussed here and support the idea that the structure of the Rieske center is widely conserved (Britt et al., 1991).

Materials and Methods

R. capsulatus strain MT1131, containing the composite plasmid pMTO-404, was grown photoheterotrophically (in anaerobiosis, with saturating light intensity) at room temperature in completely filled 1-L bottles. The growth medium used was the synthetic medium A (Sistrom, 1960), containing either 1.25 g/L of $(^{14}NH_4)_2SO_4$ or $(^{15}NH_4)_2SO_4$ (Cambridge Isotope Labs, Woburn, MA 01801), supplemented with 1 μg/mL tetracycline to assure the stable propagation of plasmids during growth. The plasmid pMTO-404 carries an expressed copy of the entire *fbc* (*pet*) operon of *R. capsulatus* and encodes the three structural genes for the Rieske iron–sulfur protein, cytochrome *b*, and cytochrome c_1 subunits of the cytochrome bc_1 complex. The strain pMTO-404/MT1131 overproduces the cytochrome bc_1 complex possibly due to the presence of multiple copies of this latter plasmid (Atta-Asafo-Adjei & Daldal, 1991).

Cells from 18 L of culture were washed in 50 mM MOPS, pH 7.0, and 100 mM KCl, and chromatophores were prepared as outlined in Dutton et al. (1975). Cytochrome bc_1 was solubilized from chromatophores using dodecyl maltoside in the presence of glycerol as follows: after washing in 50 mM Tris, pH 8.0, 100 mM NaCl, and 1 mM $MgCl_2$, chromatophores were resuspended and stirred on ice. Glycerol was added to a final concentration of 20% (v/v). The subsequent addition of detergent was calculated to result in dilution of the chromatophore suspension to 10 mg of protein/mL. Dodecyl maltoside (100 mg/mL; Anatrace Inc., Maumee, OH 43537) was added dropwise at 4 °C to achieve a final detergent/protein ratio of 1:1 (w/w) (Ljungdall et al., 1987). The complex was purified by anion exchange chromatography using DEAE-Bio-Gel A and subsequently DEAE-Sepharose CL-6B. Further purification was achieved by gel filtration chromatography with Sepharose CL-4B (Andrews et al., 1990). The enzyme was concentrated using the Amicon Centriprep 30 system.

The ENDOR spectra were recorded at $T \simeq 2$ K on a modified Varian Assoc. 35-GHz spectrometer as described previously (Gurbiel et al., 1989) except that data were stored in digital form on a PC clone using software written by Dr. R. Morse (1987).

[1] Abbreviations: ENDOR, electron nuclear double resonance; ESEEM, electron spin scho envelope modulation; BC1, cytochrome bc_1 from *Rhodobactor capsulatus*; PDO, phthalate dioxygenase from *Pseudomonas cepacia*.

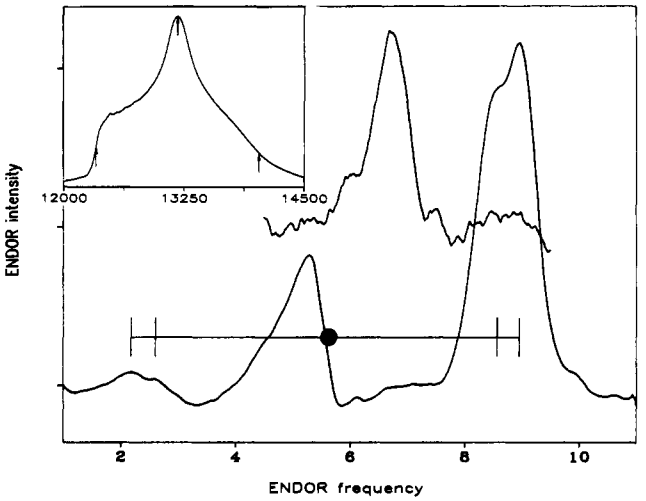

FIGURE 1: ^{15}N ENDOR spectrum of cytochrome bc_1 complex of *R. capsulatus* taken at g_{mid}. A circle (●) marks nuclear Larmor frequency of ^{15}N; braces correspond to hyperfine coupling of two nitrogens. For comparison (above) is a portion of an ^{14}N spectrum taken under similar conditions and (inset) the EPR spectrum with marked field positions corresponding to principal g values. Conditions: microwave frequency and power, 35.35 GHz, 50 μW; modulation amplitude 3.2 G; rf power 20 W; scan rate 2.5 MHz/s; 400 scans. The EPR scan time is 4 min.

The first-order ^{14}N ($I = 1$) ENDOR spectrum for a single orientation of a paramagnetic center consists, in principle, of four transitions at frequencies given by

$$\nu_{\pm,m}(^{14}N) = |\nu(^{14}N) \pm \frac{A(^{14}N)}{2} + \frac{3P(^{14}N)}{2}(2m - 1)| \quad (1)$$

where A and P are the angle-dependent ^{14}N hyperfine and quadrupole coupling constants, respectively (Abragam & Bleaney, 1970). The nuclear spin projection is $m = 1$ or 0, and $\nu(^{14}N)$ is the Larmor frequency. In contrast, a ^{15}N nucleus has $I = 1/2$ and does not exhibit a quadrupole splitting, and thus gives a two-line pattern

$$\nu_{\pm}(^{15}N) = \left|\nu(^{15}N) \pm \frac{A(^{15}N)}{2}\right| \quad (2)$$

The hyperfine couplings and Larmor frequencies of ^{14}N and ^{15}N are related by fundamental nuclear properties

$$\frac{A(^{15}N)}{A(^{14}N)} = \frac{\nu(^{15}N)}{\nu(^{14}N)} = \left|\frac{g(^{15}N)}{g(^{14}N)}\right| = 1.403 \quad (3)$$

The samples employed in this study were frozen solutions and thus contain a random distribution of protein orientations. However, spectra taken at the extreme edges of the EPR spectrum, corresponding to g_{max} and g_{min}, gave single-crystal-like ENDOR spectra (Rist & Hyde, 1970). By simulating the ENDOR spectra recorded at numerous fields (different g values) across the envelope, it is possible to evaluate the principal values of the hyperfine tensor and the three Euler angles (α, β, γ) that describe its orientation in respect to diagonal g tensor (Hoffman et al., 1984, 1985; True et al., 1988). The simulation does not use the approximate eqs 1 and 2, but rather a more exact treatment (Thuomas & Lund, 1974). In simulating ^{14}N ENDOR spectra, it was sufficient to consider only the first-order quadrupole interaction because the second-order quadrupole contributions are found to be negligibly small (Iwasaki, 1974).

Results

The Q-band ENDOR spectrum of a ^{15}N-enriched sample of BC1 taken at g_{mid} clearly shows a pair of lines at $\nu \cong 9$ MHz

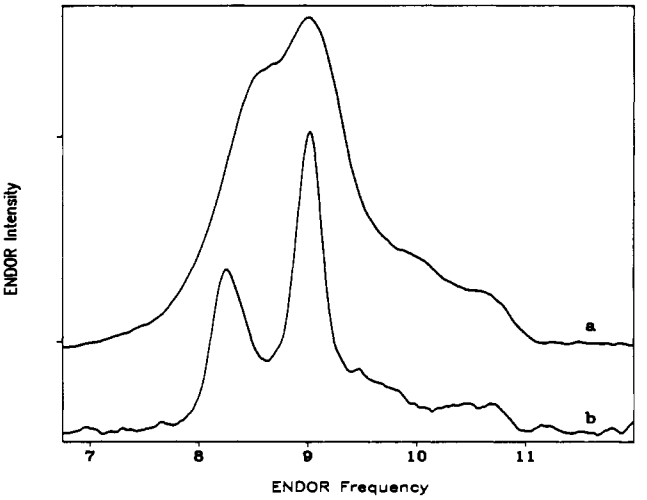

FIGURE 2: A comparison of the ^{15}N nitrogen ENDOR spectra of the Rieske iron–sulfur cluster of (a) BC1 and Rieske-type cluster of (b) PDO. Conditions are as in Figure 1.

and an additional feature at approximately 5.7 MHz (Figure 1). The latter lies almost exactly at the nuclear Larmor frequency of ^{15}N and is undoubtedly the ENDOR signal of weakly coupled nitrogen. The pair at ~9 MHz is the ν_+ branch of a ^{15}N ENDOR pattern whose low-frequency counterpart is barely detected at ~2.5 MHz. These assignments are confirmed by comparison with the ENDOR spectrum of the ^{14}N BC1 sample, which is shifted to lower frequency in agreement with eqs 1–3 (ignoring the ^{14}N quadrupole term). The big difference in signal intensities, with ν_+ much more intense than ν_-, likely reflects nuclear enhancement factors in this case. As a result, the analysis was based on the ν_+ branch of the ^{15}N ENDOR spectra.

The ^{15}N ENDOR spectrum of BC1 at g_{mid} bears a strong resemblance to the comparable spectrum of PDO (Figure 2). Although the poorly resolved pair of BC1 is sharply resolved in PDO, the peak positions correspond well. Further, in both cases there are weaker features to higher frequency of the pair and the breadth of the ENDOR pattern is essentially the same; the significance of this will be further discussed later.

To determine the number of nitrogen ligands contributing to the spectrum of Figure 2 and to evaluate their complete **A** tensor(s), single-crystal-like spectra were taken at the extreme edges of the EPR envelope and numerous spectra were taken throughout the envelope; several of those spectra are shown in Figure 3. The single-crystal-like spectrum taken at $g_{min} = 1.79$ shows a strong unsymmetric single peak with a shoulder at high frequency. As the observing g value is increased (magnetic field decreased), (i) the peak moves toward lower frequency, (ii) the shoulder at the lower frequency side of the peak gradually evolves into the separate peak seen at g_{mid}, and (iii) a much weaker shoulder appears at the high-frequency edge of the pattern, the breadth of the pattern reaching its maximum at g_{mid}. As the observing g value is further increased, the strong doublet moves back toward higher frequency, and the weak high-frequency shoulder retreats to lower frequency. Finally, two nitrogen peaks remain resolved at the *extreme* low-field edge of the EPR envelope; this observation of two ν_+ peaks at a rigorously single-crystal-like field value proves that the spectrum is the superposition of signals from two different nuclei.

The ENDOR spectra for different g values across the EPR envelope were simulated as the sum of responses from two ^{15}N ligands. The starting values for the simulation were the hyperfine coupling tensors reported for the Rieske-type cluster

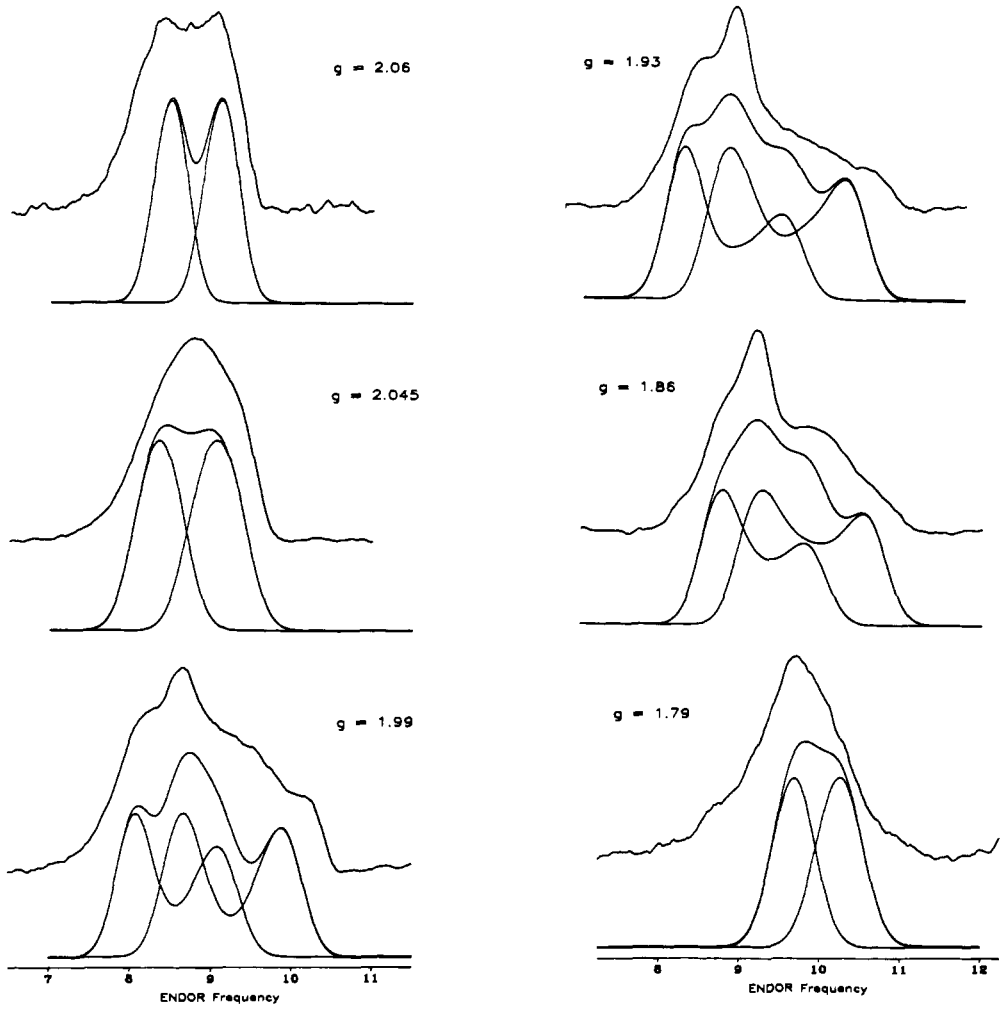

FIGURE 3: The ν_+ branch of the ^{15}N ENDOR spectra of BC1 taken at fields (g values) throughout the EPR envelope; simulations were calculated as described in the text with tensors given in Table I. Conditions are as in Figure 1.

of phthalate dioxygenase (PDO) from *P. cepacia* (Gurbiel et al., 1989). These values were adjusted to achieve agreement with experiment as described earlier. The tensors given in Table I produce the simulations shown in Figure 3; Figure 4 shows the full set of experimental and calculated peak (or shoulder) positions.

The simulation procedure that yielded the hyperfine tensor parameters listed in Table I takes into account both the experimental ν_+ frequencies as summarized in Figure 4 and the general shape of the ν_+ ENDOR features (Figure 3), namely, the fact that the strongest feature(s) is (are) to lower frequency and is (are) accompanied by a weaker shoulder to higher frequency. Reproducing this shape strongly constrains the values of parameters that were used for a simulation. As a result, the simulations are not as successful as those for the Rieske center of PDO (Gurbiel et al., 1989), and in particular they do not match exactly the highest frequency shoulder in the spectra (Figures 3 and 4), although in most cases the difference is 0.2–0.3 MHz or less. If one does not consider the shape of the ENDOR pattern but only its peak positions, it is possible to obtain a better fit to the frequencies of peaks and shoulders, as represented by the dotted lines in Figure 4. This procedure leaves A(1) unchanged but changes the principal values of A(2) slightly, by less than 10%; however, it gives simulations with the maximum intensity to high frequency and a weaker shoulder to lower frequency, contrary to observation (Figure 3). Only detailed studies of the orientation dependence of ENDOR intensities can determine whether the observed pattern could be reproduced by more rigorous treatment of intensities using this second pair of hyperfine tensors. For now we consider the discrepancy between the two A(2) tensors to provide a generous estimate of the uncertainty in the fit parameters for this nitrogen.

Table I: Hyperfine Tensor Principal Values (MHz) and Orientation (deg) Relative to g Tensor Principal Axes for the Histidyl–Nitrogen Ligands to the [2Fe–2S] Cluster of Cytochrome bc_1 from *R. capsulatus*[a] and Phthalate Dioxygenase from *P. cepacia*[b]

	principal values			
	BC1		PDO	
	site 1[c]	site 2[d]	site 1	site 2
$A(^{15}N)$				
A_1	5.0 (1)	6.0 (2)	4.6 (2)	6.4 (1)
A_2	5.6 (1)	7.4 (5)	5.4 (1)	7.0 (1)
A_3	8.4 (1)	9.7 (2)	8.1 (1)	9.8 (2)
Euler angles[e]				
α	0 (10)	0 (10)	0 (30)	0 (10)
β	38[f] (3)	40[g] (40)	35 (5)	50 (5)
γ	–[h]	–[h]	0 (10)	0 (30)

[a] This work. The absolute signs of the A_i are not determined; for an individual site, all have the same sign. [b] Gurbiel et al. (1989). [c] Uncertainties represent precision in the simulations, not necessarily the accuracy. [d] As described in the text, line positions but not intensities are better fit with principal values (5.8, 7.9, and 9.9 MHz) and β = 44°. The listed uncertainties reflect this discrepancy. [e] Euler angles relate the A tensor to the reference g frame; they are discussed under Materials and Methods. [f] Upper limit. [g] Lower limit. [h] This angle cannot be determined solely from data on the ^{15}N protein.

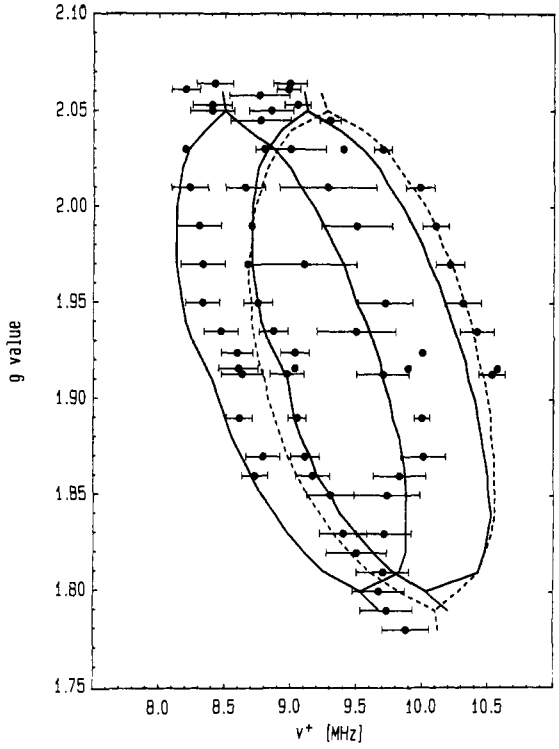

FIGURE 4: Plot of the frequency of the ν_+ ENDOR features versus the observing g value (static field). The error bars represent approximately one-third of the signal line width. Solid lines represent theoretical values calculated with hyperfine tensor parameters given in Table I and determined by optimizing both the peak positions and the overall shape of the ENDOR pattern. The dotted line drawn for the A(2) tensor was calculated with parameters that take into account only peak positions but not the shape of the pattern.

The ^{15}N hyperfine tensors for the two ligands to the Rieske $[2Fe-2S]^{+1}$ cluster are similar but not identical (Table I). Both have large isotropic components, which proves that the nitrogens are coordinated to an iron ion of the cluster.[2] Both have roughly axial symmetry with the unique axis, A_3 assigned to the Fe–N bond; we recognize, but for now ignore the possibility, that bending of the Fe–N bond might cause a misalignment of A_3 and the Fe–N vector. A closer look at the principal values of the tensors reveals that the A(1) tensor is close to axial but that the A(2) tensor is not; as one measure of the deviation from axial symmetry, the ratio $R = (A_2 - A_1)/[A_3 - (A_1 + A_2)/2] = 0.19$ and 0.47 for A(1) and A(2), respectively. The angle between the g_3 axis and the Fe–N vector, described by the Euler angle β, within error is the same for both nuclei. However, it may be important to point out that it was impossible to simulate the experimental spectra with these angles identical.

Comparison of the ENDOR spectra and the ^{15}N hyperfine tensors of BC1 and PDO shows that the principal values for A(1) are indistinguishable for the two proteins; those for A(2) differ from those for A(1) but again are quite similar for the two proteins. However, it does appear that A(2) for PDO is more axial ($R = 0.19$) than that for BC1 ($R = 0.47$). The g_3–Fe–N angle of both ligands for the BC1 protein (within the error) is the same $\beta \simeq 40°$, whereas for the two ligands of the PDO protein the angles are distinctly different, $\beta \simeq 35°$ and 50°. The sum of the two angles, $\beta(1) + \beta(2)$, is

[2] Some ENDOR data on aconitase was tentatively interpreted in terms of a large isotropic hyperfine coupling to a ^{14}N not coordinated to the [4Fe–4S] cluster (Werst et al., 1990). Recently this interpretation has been shown to be incorrect (Houseman et al., 1991).

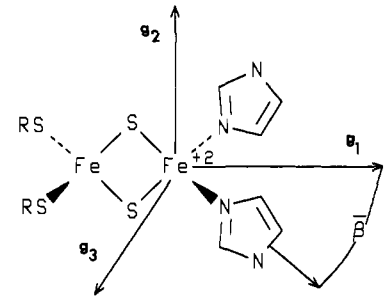

FIGURE 5: Proposed geometry of the [2Fe–2S] cluster of the Rieske protein. Four protein ligands and two iron ions lie in the g_1–g_3 plane. Further details are given in the text.

comparable, however. A second noticeable difference between the ENDOR spectra of those two iron–sulfur clusters is that the line width of the signal of the BC1 Rieske protein is at least twice that of the Rieske-type center of PDO.

Given the nearly identical hyperfine tensors for the N ligands of PDO and BC1, the arguments given in our previous paper show that we may take the geometric structures of both clusters to be essentially the same as deduced for the Rieske-type [2Fe–2S] cluster of *P. cepacia*, with both nitrogen ligands bound to the ferrous ion. This make it possible to calculate the fundamental hyperfine tensor **a** that describes the interaction of the nitrogen with the spin of the isolated Fe^{2+} ion (Gibson et al., 1966; Sands et al., 1975).

The correlation between the measured hyperfine tensor A(i), $i = 1$ or 2, describing the interaction of a nitrogen coordinated to the Fe^{2+} ion with the total spin of the spin-coupled $[Fe^{2+},Fe^{3+}]$ pair, and the fundamental hyperfine tensor **a**(i) is given by

$$\mathbf{a}(i) = -3\mathbf{A}(i)/4 \qquad (4)$$

As described previously (Gurbiel et al., 1989), knowing the hyperfine coupling **a**, one can calculate the fraction of unpaired electron spin that resides in the 2s orbital of nitrogen, f_{2s}. For the BC1 those values are $f_{2s}(1) \cong 1.7\%$ and $f_{2s}(2) \cong 2\%$, as compared to $f_{2s}(1) \cong 1.5\%$ and $f_{2s}(2) \cong 2\%$ for PDO. These values are quite similar to that reported for histidine coordinated as the axial ligand of the high-spin Fe^{3+} ion in aquometmyoglobin $f_{2s} \cong 3\%$ (Scholes et al., 1982). In the case of PDO, selective labeling proved that the nitrogen was associated with histidine imidazole, and the similarity of the hyperfine tensor values indicates that the same is true here.

The results presented above further indicate that the overall geometry of the [2Fe–2S] cluster is similar for both the Rieske and Rieske-type protein (Figure 5). The four protein-donated ligands and two iron ions lie in the g_1–g_3 plane with the g_1 or g_3 axes predicted to lie in the direction of the Fe–Fe vector (Bertrand et al., 1985). Although ^{57}Fe ENDOR studies or single-crystal measurements will be required to resolve that ambiguity, the crystal-field analysis of the g values for [2Fe–2S] clusters with $g_{av} \cong 1.91$ suggested that the g_3 tensor axis lies along the Fe–Fe vector, unlike the ferredoxin-type clusters with $g_{av} = 1.96$, where the Fe–Fe vector corresponds to g_1 (Bertrand et al., 1985). In the former case the bite angle subtended by the two Fe–N vectors is $\beta(1) + \beta(2)$ and lies in the range 80°–85° for both proteins, while in the latter the bite angle is $\pi - [\beta(1) + \beta(2)]$ and lies in the range 95°–100°. For PDO, the torsion angle γ of the imidazole ring about the Fe–N vector was also estimated from ^{14}N ENDOR data.

DISCUSSION

The present results have proven that the coordination of the [2Fe–2S] cluster of the Rieske protein of cytochrome bc_1

complex from *R. capsulatus* involves two nitrogenous ligands. Comparison with data for the Rieske-type cluster of PDO shows a close similarity which indicates (1) both coordinated nitrogens are from histidines and (2) both are coordinated to the Fe^{2+} ion.

However, the geometries of the two clusters are noticeably different. The two g_3–Fe–N bond angles are essentially equal in the cluster of the cytochrome bc_1 complex, but they are distinctly different in PDO. In short, the structure of the BC1 cluster is more symmetric than that of the PDO cluster. Nevertheless, in both cases there is an asymmetry at the Fe^{2+} ion: the bonding parameters of the two nitrogens in a given cluster are significantly different for both BC1 and PDO. As a further difference, it appears that the structural heterogeneity of the cluster, as measured by the ENDOR line widths, is greater for BC1 than for PDO.

As a functional point of interest, the same ligation scheme of PDO and BC1 does not lead to comparable electrochemistries for their [2Fe–2S] centers. The electrochemical midpoints of Rieske-type bacterial dioxygenase and Rieske protein in cytochrome bc_1 are quite different [−100 to 0 mV and +140 to +330 mV, respectively (Prince et al., 1975; Geary et al., 1984)], leading to the supposition that the differences in cluster geometry, active site solvent chemistry, or in protein environment are more important in determining the electron affinities of [2Fe–2S] clusters. The factors contributing to E_m values of heme proteins have been explored by Kassner (1972), who has concluded that solvent and protein constraints were of greater importance in determining electrochemistry.

References

Abragam, A., & Bleaney, B. (1970) *Electron Paramagnetic Resonance of Transition Ions*, Clarendon Press, Oxford.

Andrews, K. M., Crofts, A. R., & Gennis, R. B. (1990) *Biochemistry 29*, 2645–2651.

Atta-Asafo-Adjei, E., & Daldal, F. (1991) *Proc. Natl. Acad. Sci. U.S.A. 88*, 492–496.

Batie, C. J., La Haie, E., & Ballou, D. P. (1987) *J. Biol. Chem. 262*, 1510–1518.

Bertrand, P., Guigliarelli, B., Gayda, J.-P., Beardwood, P., & Gibson, J. F. (1985) *Biochim. Biophys. Acta 831*, 261–266.

Blumberg, W. E., & Peisach, J. (1974) *Arch. Biochem. Biophys. 162*, 502–512.

Bowyer, J. R., Dutton, P. L., Prince, R. C., & Croft, A. R. (1980) *Biochim. Biophys. Acta 592*, 445–460.

Britt, R. D., Sauer, K., Klein, M. P., Knaff, D. B., Kriauciunas, A., Yu, C.-A., Yu, L., & Malkin, R. (1991) *Biochemistry 30*, 1892–1901.

Brustolon, M., & Serge, U. (1989) *Advanced EPR. Applications in Biology and Biochemistry* (Hoff, A. J., Ed.) pp 593–614, Elsevier, Amsterdam.

Cline, J. F., Hoffman, B. M., Mims, W. B., LaHaie, E., Ballou, D. P., & Fee, J. A. (1985) *J. Biol. Chem. 260*, 3251–3254.

Davidson, E., & Daldal, F. (1987) *J. Mol. Biol. 195*, 13–24.

Dutton, P. L., Petty, K. M., Bonner, H. S., & Morse, S. D. (1975) *Biochim. Biophys. Acta 387*, 536–556.

Fee, J. A., Findling, K. L., Yoshida, T., Hille, R., Tarr, G. E., Hearshen, D. O., Dunham, W. R., Day, E. P., Kent, T. A., & Münck, E. (1984) *J. Biol. Chem. 259*, 124–133.

Fukuyama, K., Hase, T., Matsumoto, S., Tsukihara, T., Katsube, J., Tanaka, N., Kakudo, M., Wada, K., & Matsubara, H. (1980) *Nature 286*, 522–524.

Gatti, D. L., Meinhardt, S. W., Ohnishi, T., & Tzagoloff, A. (1989) *J. Mol. Biol. 205*, 421–435.

Geary, P. J., Saboowalla, F., Patil, D., & Cammack, R. (1984) *Biochem. J. 217*, 667–673.

Gibson, J. F., Hall, D. O., Thornley, J. H. M., & Whatley, F. R. (1966) *Proc. Natl. Acad. Sci. U.S.A. 56*, 987–990.

Gurbiel, R. J., Batie, C. J., Sivaraja, M., True, A. E., Fee, J. A., Hoffman, B. M., & Ballou, D. (1989) *Biochemistry 28*, 4861–4871.

Harnish, U., Weiss, H., & Sebald, W. (1985) *Eur. J. Biochem. 149*, 95–99.

Hauska, G., Hurt, E., Gabellini, N., & Lockau, W. (1983) *Biochim. Biophys. Acta 726*, 97–133.

Hoffman, B. M., Martinsen, J., & Venters, R. A. (1984a) *J. Magn. Reson. 59*, 110–123.

Hoffman, B. M., Martinsen, J., & Venters, R. A. (1984b) *J. Magn. Reson. 62*, 537–542.

Hoffman, B. M., Gurbiel, R. J., Werst, M. M., & Sivaraja, M. (1989) *Advanced EPR. Applications in Biology and Biochemistry* (Hoff, A. J., Ed.) pp 541–591, Elsevier, Amsterdam.

Houseman, A. L. P., Byung-Ha, O., Kennedy, M. C., Fan, C., Werst, M. M., Beinert, H., Markley, J. L., & Hoffman, B. M. (1991) *Biochemistry* (submitted).

Iwasaki, M. (1974) *J. Magn. Reson. 16*, 417–423.

Kassner, R. J. (1972) *Proc. Natl. Acad. Sci. U.S.A. 69*, 2263–2267.

Ljungdahl, P., Pennoyer, J. D., Robertson, D. E., & Trumpower, B. L. (1987) *Biochim. Biophys. Acta 891*, 227–241.

Meinhardt, S. W., Yang, X., Trumpower, B. L., & Ohnishi, T. (1987) *J. Biol. Chem. 262*, 8702–8706.

Morse, P. D., II (1987) *Biophys. J. 51*, 440a.

Powers, L., Schägger, H., von Jagow, G., Smith, J., Chance, B., & Ohnishi, T. (1989) *Biochem. Biophys. Acta 975*, 293–298.

Prince, R. C., Lindsay, J. G., & Dutton, P. L. (1975) *FEBS. Lett. 51*, 108–111.

Rieske, J. S. (1976) *Biochim. Biophys. Acta 456*, 195–247.

Rist, G. H., & Hyde, J. S. (1970) *J. Chem. Phys. 52*, 4633–4643.

Sands, R. H., & Dunham, W. R. (1975) *Q. Rev. Biophys. 7*, 443–504.

Scholes, C. P., Lapidot, A., Mascarenhas, R., Inubushi, T., Isaacson, R. A., & Feher, G. (1982) *J. Am. Chem. Soc. 104*, 2724–2735.

Sistrom, W. R. (1960) *J. Gen. Microbiol. 22*, 778–785.

Telser, J., Hoffman, B. M., LoBrutto, R., Ohnishi, T., Tsai, A.-L., Simkin, D., & Palmer, G. (1987) *FEBS Lett. 214*, 117–121.

Thuomas, K.-A., & Lund, A. (1974) *J. Magn. Reson. 18*, 12–21.

True, A. E., Nelson, M. J., Venters, R. A., Orme-Johnson, W. A., & Hoffman, B. M. (1988) *J. Am. Chem. Soc. 110*, 1935–1943.

Trumpower, B. L. (1981) *Biochim. Biophys. Acta 639*, 129–155.

Trumpower, B. L. (1990) *Microbiol. Rev. 54*, 101–129.

Werst, M. M., Kennedy, M. C., Houseman, A. L. P., Beinert, H., & Hoffman, B. M. (1990) *Biochemistry 29*, 10533–10540.

Yasunobu, K. T., & Tanaka, M. (1973) in *Iron–sulfur protein II* (Lovenberg, W., Ed.) pp 27–130, Academic Press, New York.